Estimating intercellular surface tension by laser-induced cell fusion

Masashi Fujita[1,2] and Shuichi Onami[1,2*]

Affiliations:

[1]Laboratory for Developmental Dynamics, RIKEN Quantitative Biology Center

[2]Developmental Systems Modeling Team, Advanced Computational Sciences Department, RIKEN Advanced Science Institute

2-2-3 Minatojima-minamimachi, Chuo-ku, Kobe, Hyogo 650-0047, Japan

[*]Corresponding author: Shuichi Onami

Laboratory for Developmental Dynamics, RIKEN Quantitative Biology Center

2-2-3 Minatojima-minamimachi, Chuo-ku, Kobe, Hyogo 650-0047, Japan

Phone: +81-78-306-3440

Fax: +81-78-306-3442

E-mail: sonami@riken.jp

Abstract

Intercellular surface tension is a key variable in understanding cellular mechanics. However, conventional methods are not well suited for measuring the absolute magnitude of intercellular surface tension because these methods require determination of the effective viscosity of the whole cell, a quantity that is difficult to measure. In this study, we present a novel method for estimating the intercellular surface tension at single-cell resolution. This method exploits the cytoplasmic flow that accompanies laser-induced cell fusion when the pressure difference between cells is large. Because the cytoplasmic viscosity can be measured using well-established technology, this method can be used to estimate the absolute magnitudes of tension. We applied this method to two-cell-stage embryos of the nematode *Caenorhabditis elegans* and estimated the intercellular surface tension to be in the 30–90 μN/m range. Our estimate was in close agreement with cell–medium surface tensions measured at single-cell resolution.

Text

During embryogenesis, cells migrate and undergo morphological changes and rearrangements. These dynamic processes are mediated by the contractility of the cell cortex and adhesion between cells. From the viewpoint of mechanics, the contributions of contractility and adhesion can be combined into a single quantity: cell surface tension [1-4]. Therefore, the cell surface tension is critical for understanding the mechanical aspects of embryogenesis. Cell surfaces can be classified on the basis of milieu, such as cell–medium and cell–cell interfaces. Among these, cell–cell interfaces are the most important for developmental biology. Thus, the cell surface tension at these interfaces is a matter of interest.

However, measurement of the intercellular surface tension is not straightforward because the cell–cell interfaces are physically inaccessible. To circumvent this difficulty, current measurement methods employ a velocity-based strategy. In this strategy, tension-driven movements of cells (or subcellular structures) are observed and their velocities are computed. Because cell movements are in an overdamped regime and forces acting on the cell are proportional to the velocity in this regime, the relative magnitudes of tension can be inferred. An excellent example of this strategy is laser microsurgery [5-10]. Laser microsurgery, which monitors the recoil of cells or the cell cortex after laser ablation, has

provided significant insights into developmental mechanics. Other velocity-based methods observe spontaneous cell movements [11] or responses to externally applied stresses [12].

However, despite its successful applications in developmental biology, the velocity-based strategy has one problem that remains unsolved: it is difficult to measure the absolute magnitudes of intercellular surface tension. Theoretically, because of the overdamped dynamics, the absolute magnitude can be estimated by multiplying the movement velocity by the viscosity of relevant materials. However, the problem is that the relevant viscosity is hard to measure experimentally. This is particularly true for effective viscosity of the whole cell, a quantity that rules all aspects of cell movements [13, 14]. Several researchers have assumed that the effective viscosity is equal to the cytoplasmic viscosity [9, 11, 12]. However, the validity of this assumption is uncertain because the effective viscosity could be produced not only by the cytoplasm but also by the cell cortex [15], nuclei [16, 17], and extracellular components [18].

The abovementioned drawback of the velocity-based strategy could be solved by focusing on specific cellular components that are more amenable to rheological measurements. The cytoplasm is constitutively much simpler than the whole cell, and its viscoelasticity can be evaluated by microrheological methods [19-23]. On the basis of this

idea, we developed a novel method that analyzed the cytoplasmic velocity for estimating intercellular surface tensions.

This method focuses on specific situations when two cells in contact have a large difference in their intracellular hydrostatic pressures. This pressure difference will have two consequences: first, the cell–cell interface will be curved like an arc (Fig. 1 A); second, the cytoplasm will flow between the cells when their interface is perforated (Fig. 1 B). By relating these two phenomena, our method estimates the surface tension at the interface.

The curvature of a cell–cell interface is related to the intercellular surface tension and the pressure difference by Laplace's law:

$$\Delta P = \frac{2\gamma}{R}, \qquad (1)$$

where ΔP is the pressure difference, γ is the intercellular surface tension, and R is the interface curvature radius (Fig. 1 A). Therefore, γ can be determined if the values of ΔP and R are known. The value of R can be obtained by curve fitting using microscopic images.

We used laser-induced cell fusion to perforate the cell–cell interface. Two cells in contact can be selectively fused by irradiating their interface with a UV laser [24-26]. Upon cell fusion, the cytoplasm of the cell with higher hydrostatic pressure will flow into the cell with lower pressure (Fig. 1 B). The flow velocity is related to the pressure difference ΔP and

the cytoplasmic viscoelasticity. To elucidate this relationship, computer simulation of fluid dynamics will be required for the general situation. However, the cytoplasm of some specific cell types can be approximated as simple Newtonian fluids, and we consider these situations hereafter.

We modeled the cytoplasmic flow as an incompressible fluid flowing through a circular pore in a thin planar wall. Many cell-scale phenomena are found in the low Reynolds number regime [27], and the flow in this regime follows Sampson's law [28], which states that the pressure difference across the wall is

$$\Delta P = 3\pi \frac{v\mu}{c}, \qquad (2)$$

where v is the mean flow velocity through the pore, μ is the shear viscosity of the fluid, and c is the pore radius. The intercellular surface tension γ can be estimated by combining Eqs. 1 and 2.

We applied this theory to the two-cell-stage embryos of *C. elegans*, which is the simplest system in terms of cell–cell interfaces (Fig. 2 A). The viscoelasticity of their cytoplasm was previously investigated by Daniels *et al*. [22]. The cytoplasm had negligible elasticity, suggesting that it satisfied Newtonian fluidity, a prerequisite for using Eq. 2. The cytoplasmic viscosity was $\mu = 10 \pm 1$ Poise. Although Daniels *et al.* studied one-cell-stage

embryos, they found no significant difference between the anterior and posterior regions, which are the immediate predecessors of two-cell-stage blastomeres. Therefore, we assumed that μ in the two-cell stage was identical to that in the one-cell stage.

The two-cell-stage embryo comprises an anterior AB cell and a posterior P_1 cell, and its shape is nearly symmetric around the anterior–posterior axis. The cell–cell interface is initially flat; however, it gradually forms a bulge extending from AB to P_1. Application of laser irradiation to this interface causes fusion of the two cells and is accompanied by cytoplasmic flow from AB to P_1 [24].

We performed this fusion experiment to estimate the intercellular surface tension (n = 9). Immediately after laser irradiation, a flow of cytoplasmic granules was observed near the irradiated sites (Fig. 2 B and Movie S1 in the Supporting Material). This flow was directed from AB to P_1, consistent with a previous report [24]. The flow gradually attenuated, although it continued until approximately 50 s. The membrane pore size was initially small, but gradually enlarged, indicating that contractile forces were acting on the cell–cell interfaces. These interfaces, which were curved at the onset of fusion, became flat after 30 s.

We quantified the flow velocities, pore radii, and curvature radii of these interfaces from the 9 image sequences and computed the sample means and SEMs (mean ± SEM). The

flow velocity v was maximal at the onset of fusion (Fig. 3 A), with a value of 0.9 ± 0.1 μm/s. The pore radius c had a minimum value of 2.6 ± 0.2 μm at the onset of fusion (Fig. 3 B). The curvature radius R was initially 32 ± 2 μm and then gradually increased for 25 s (Fig. 3 C). 30 s after the onset of fusion, both the mean and SEM values of R showed a sudden increase, presumably because of the flatness of the interface. Because the curvature estimation for a nearly flat surface is technically difficult, we believe that these values of R after 30 s may contain large computational artifacts. Therefore, the latter half of the time course requires careful interpretation.

We then estimated the pressure difference ΔP from Eq. 2. The estimated ΔP had a maximal value of 3.4 ± 0.4 Pa at the onset of fusion and then gradually decreased (Fig. 3 D). The intercellular surface tension γ was then estimated by substituting the values of ΔP and R into Eq. 1. The intercellular surface tension was estimated to be $\gamma = 51 \pm 5$ μN/m and was within the 39–50 μN/m range over the next 40 s (Fig. 3 E). Correction coefficients were introduced to take into account the possible effects of membrane geometry, and the estimates of γ were widened to the 27–93 μm range (for details, see the Supporting Material).

Our estimates were compared with the reported values of cell surface tensions and were found to be similar to those of cell–medium interfaces, but not to those of cell-cell

interfaces. For example, cell–medium surface tensions of fish cells were in the 30–80 μN/m range (Figure 2d in [29]), whereas those of neutrophils were in the 10–30 μN/m range [30, 31]. In contrast, the intercellular surface tension of fly epithelia corresponded to 330 μN/m [9], while that of a cell aggregate was estimated to be 22.9 mN/m [12]. These large discrepancies between intercellular surface tensions could be attributable to sample differences or to differences in the assumed viscosity values.

We used a value of 10 Poise for viscosity, whereas previous papers used values of 100 and 9600 Poise. Their ratio matches up well with the ratio of the measured intercellular surface tensions: 27–93:330:22900 μN/m. This consideration reconfirms the importance of using an accurate viscosity value. It might be argued that viscoelasticity might have a length-scale dependency because the cytoplasm is highly inhomogeneous. However, in the case of *C. elegans* embryos, the probe size of Daniels *et al.* (100 nm) will be larger than the length scale of non-uniformity in the cytoplasm. This is because actin meshwork, which plays the central role in cell rheology, apparently absent from the embryo cytoplasm [32]. Even if the meshwork exists, its length scale is ~50 nm [33]. Therefore, the value of viscosity we used would reflect bulk viscosity of the cytoplasm in the nematode embryos.

One drawback of our method is the assumption that the cytoplasm is a Newtonian

fluid. Although generalization to non-Newtonian fluids might be possible with the aid of computational fluid dynamics, this Newtonian assumption could be practically limiting. However, undifferentiated cells have more fluid-like behavior than differentiated cells [22, 23]. Furthermore, weak elasticity has little effect on Sampson's law [34]. Therefore, our method might be applicable to early embryogenesis, even in its current state.

Another drawback of our method is that it is applicable only to cell–cell interfaces that are curved because of the large pressure differences involved. This raises a question regarding which part of our estimation procedure will face obstacles if the pressure difference is small. In our results, the magnitudes of ΔP became significantly small at 30 s or later (Fig. 3 D); however, we could still detect the cytoplasmic flow (Fig. 3 A). In contrast, the estimation of R became highly unstable when the interface was nearly flat (Fig. 3 C). This suggests that the current limitation of our method primarily arises from the inability to measure R accurately for weakly curved interfaces. The application range of our method may be extended using improved microscopy for cell-shape imaging or numerical algorithms for curvature computation.

In conclusion, we have presented a novel method for estimating the intercellular surface tension. This method has single-cell resolution and allows estimation of the absolute

magnitude of this tension. Because the applicability of our method is currently limited, further study will be required to extend its areas of application.

Acknowledgments

The N2 strain was provided by the *Caenorhabditis* Genetics Center, which is funded by the NIH National Center for Research Resources (NCRR). This study was supported by grants from KAKENHI (Grant-in-Aid for Scientific Research) on the 'Systems Genomics' Priority Area from the Ministry of Education, Culture, Sports, Science, and Technology of Japan.

References

[1] Lecuit T, Lenne P-F. Cell surface mechanics and the control of cell shape, tissue patterns and morphogenesis. Nat Rev Mol Cell Biol. 2007 Aug 1;8(8):633-44.

[2] Mammoto T, Ingber DE. Mechanical control of tissue and organ development. Development. 2010 May 1;137(9):1407-20.

[3] Montell DJ. Morphogenetic cell movements: diversity from modular mechanical properties. Science. 2008 Dec 5;322(5907):1502-5.

[4] Manning ML, Foty RA, Steinberg MS, Schoetz E-M. Coaction of intercellular adhesion and cortical tension specifies tissue surface tension. Proc Natl Acad Sci USA. 2010 Jun 28;107(28):12517–22.

[5] Hutson M, Tokutake Y, Chang M, Bloor J, Venakides S, Kiehart D, et al. Forces for morphogenesis investigated with laser microsurgery and quantitative modeling. Science. 2003;300(5616):145.

[6] Farhadifar R, Röper J-C, Aigouy B, Eaton S, Jülicher F. The influence of cell mechanics, cell-cell interactions, and proliferation on epithelial packing. Curr Biol. 2007 Dec 18;17(24):2095-104.

[7] Rauzi M, Verant P, Lecuit T, Lenne P-F. Nature and anisotropy of cortical forces orienting Drosophila tissue morphogenesis. Nat Cell Biol. 2008 Nov 2;10(12):1401 - 10.

[8] Ma X, Lynch HE, Scully PC, Hutson MS. Probing embryonic tissue mechanics with laser hole drilling. Phys Biol. 2009 Jan 1;6(3):036004.

[9] Hutson MS, Veldhuis J, Ma X, Lynch HE, Cranston PG, Brodland GW. Combining laser microsurgery and finite element modeling to assess cell-level epithelial mechanics. Biophysical Journal. 2009 Dec 16;97(12):3075-85.

[10] Mayer M, Depken M, Bois JS, Jülicher F, Grill SW. Anisotropies in cortical tension reveal the physical basis of polarizing cortical flows. Nature. 2010 Nov 1;467(7315):617-21.

[11] Brodland GW, Conte V, Cranston PG, Veldhuis J, Narasimhan S, Hutson MS, et al. Video force microscopy reveals the mechanics of ventral furrow invagination in Drosophila. Proc Natl Acad Sci USA. 2010 Dec 21;107(51):22111-6.

[12] Yang J, Brodland GW. Estimating interfacial tension from the shape histories of cells in compressed aggregates: a computational study. Ann Biomed Eng. 2009 Feb 13;37(5):1019-27.

[13] Chen HH, Brodland GW. Cell-level finite element studies of viscous cells in planar aggregates. J Biomech Eng. 2000 Aug 1;122(4):394-401.

[14] Cranston PG, Veldhuis JH, Narasimhan S, Brodland GW. Cinemechanometry (CMM): A

Method to Determine the Forces that Drive Morphogenetic Movements from Time-Lapse Images. Ann Biomed Eng. 2010 Sep 8;38(9):2937-47.

[15] Zhou J, Kim HY, Davidson LA. Actomyosin stiffens the vertebrate embryo during crucial stages of elongation and neural tube closure. Development. 2009 Feb 15;136(4):677-88.

[16] Guilak F, Tedrow JR, Burgkart R. Viscoelastic Properties of the Cell Nucleus. Biochemical and biophysical research communications. 2000 Mar 1;269(3):781-6.

[17] Caille N, Thoumine O, Tardy Y, Meister JJ. Contribution of the nucleus to the mechanical properties of endothelial cells. J Biomech. 2002;35(2):177-87.

[18] Ebihara T, Venkatesan N, Tanaka R, Ludwig MS. Changes in extracellular matrix and tissue viscoelasticity in bleomycin-induced lung fibrosis. Temporal aspects. American journal of respiratory and critical care medicine. 2000;162(4):1569.

[19] Bausch AR, Möller W, Sackmann E. Measurement of local viscoelasticity and forces in living cells by magnetic tweezers. Biophysical Journal. 1999 Jan 1;76(1 Pt 1):573-9.

[20] Tseng Y, Kole TP, Wirtz D. Micromechanical mapping of live cells by multiple-particle-tracking microrheology. Biophysical Journal. 2002 Dec 1;83(6):3162-76.

[21] Tolić-Nørrelykke IM, Munteanu E-L, Thon G, Oddershede L, Berg-Sørensen K. Anomalous diffusion in living yeast cells. Phys Rev Lett. 2004 Aug 13;93(7):078102.

[22] Daniels BR, Masi BC, Wirtz D. Probing single-cell micromechanics in vivo: the microrheology of C. elegans developing embryos. Biophys J. 2006 Jun 15;90(12):4712-9.

[23] Daniels BR, Hale CM, Khatau SB, Kusuma S, Dobrowsky TM, Gerecht S, et al. Differences in the Microrheology of Human Embryonic Stem Cells and Human Induced Pluripotent Stem Cells. Biophysical Journal. 2010 Jan 12;99(11):3563-70.

[24] Schierenberg E. Altered cell-division rates after laser-induced cell fusion in nematode embryos. Dev Biol. 1984;101(1):240-5.

[25] Wiegand R, Weber G, Zimmermann K, Monajembashi S, Wolfrum J, Greulich KO. Laser-induced fusion of mammalian cells and plant protoplasts. J Cell Sci. 1987 Sep 1;88(2):145-9.

[26] Irle T, Schierenberg E. Developmental potential of fused Caenorhabditis elegans oocytes: generation of giant and twin embryos. Dev Genes Evol. 2002 Jul 1;212(6):257-66.

[27] Purcell EM. Life at low Reynolds number. Am J Phys. 1977;45(1):3-11.

[28] Happel J, Brenner H. Low Reynolds number hydrodynamics: with special applications to particulate media. The Hague: Martinus Nijhoff Publishers; 1983.

[29] Krieg M, Arboleda-Estudillo Y, Puech P-H, Käfer J, Graner F, Müller DJ, et al. Tensile forces govern germ-layer organization in zebrafish. Nat Cell Biol. 2008 Apr 1;10(4):429-36.

[30] Hochmuth RM. Micropipette aspiration of living cells. J Biomech. 2000 Jan 1;33(1):15-22.

[31] Lomakina EB, Spillmann CM, King MR, Waugh RE. Rheological analysis and measurement of neutrophil indentation. Biophys J. 2004 Oct 28;87(6):4246-58.

[32] Strome S. Fluorescence visualization of the distribution of microfilaments in gonads and early embryos of the nematode Caenorhabditis elegans. J Cell Biol. 1986 Dec 1;103(6 Pt 1):2241-52.

[33] Wirtz D. Particle-tracking microrheology of living cells: principles and applications. Annual Review of Biophysics. 2009 Jan 1;38:301-26.

[34] Rothstein JP, McKinley GH. The axisymmetric contraction-expansion: the role of extensional rheology on vortex growth dynamics and the enhanced pressure drop. Journal of non-newtonian fluid mechanics. 2001;98(1):33-63.

Figure legends

Figure 1 Schematic illustration of two cells with a large pressure difference. (A) When two cells have intracellular hydrostatic pressures of P and $P + \Delta P$, the difference ΔP causes the cell–cell interface to become curved. The curvature radius R is determined from ΔP and the intercellular surface tension γ. (B) When the two cells are fused, the pressure difference ΔP produces a cytoplasmic flow through the membrane pore. The flow velocity is denoted by v.

Figure 2 (A) Differential interference contrast image of a two-cell-stage embryo of *C. elegans* at 8 min after the onset of the two-cell stage. The anterior is oriented to the left. The larger anterior cell is AB, and the smaller posterior cell is P_1. Scale bar = 10 μm. (B) Cytoplasmic flow immediately after cell fusion. Scale arrow = 1 μm/s.

Figure 3 Measured and estimated quantities as a function of time after the onset of cell fusion. (A) Flow velocity. (B) Membrane pore radius. (C) Interface curvature radius (D) Pressure difference between AB and P_1. (E) Intercellular surface tension. Error bars indicate SEMs of 9 samples.

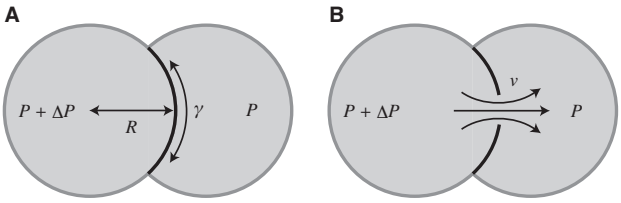

Figure. 1

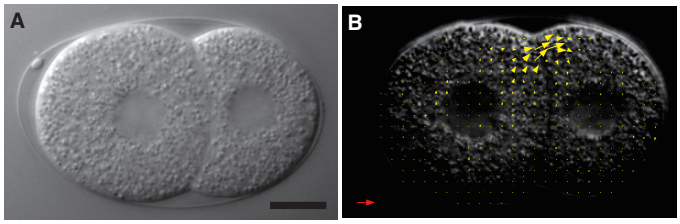

Figure. 2

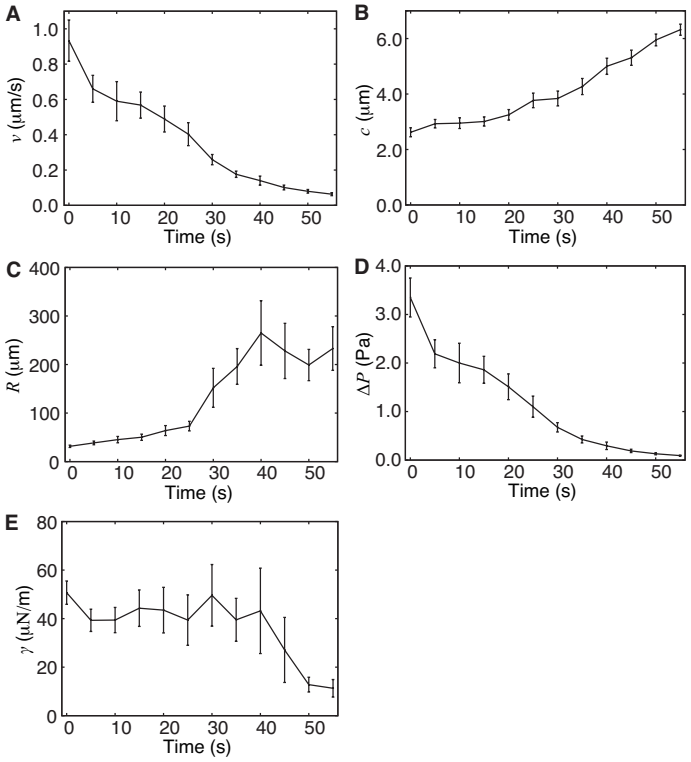

Figure. 3